

Vertically integrated metal-clad/silicon dioxide-shell microtube arrays for high-spatial-resolution light stimuli in saline

M. Sakata, T. Nakamura, T. Matsuo, A. Goryu, M. Ishida, and T. Kawano

Citation: *Applied Physics Letters* **104**, 164101 (2014); doi: 10.1063/1.4871710

View online: <http://dx.doi.org/10.1063/1.4871710>

View Table of Contents: <http://scitation.aip.org/content/aip/journal/apl/104/16?ver=pdfcov>

Published by the *AIP Publishing*

Articles you may be interested in

[The role of group index engineering in series-connected photonic crystal microcavities for high density sensor microarrays](#)

Appl. Phys. Lett. **104**, 141103 (2014); 10.1063/1.4871012

[Optical loss in silicon microphotonic waveguides induced by metallic contamination](#)

Appl. Phys. Lett. **92**, 131108 (2008); 10.1063/1.2903714

[Optical improvement of photonic devices fabricated by Ga + focused ion beam micromachining](#)

J. Vac. Sci. Technol. B **25**, 1609 (2007); 10.1116/1.2770741

[Microfabricated Sr Ti O 3 ridge waveguides](#)

Appl. Phys. Lett. **86**, 221106 (2005); 10.1063/1.1942634

[Inductively coupled plasma etching for arrayed waveguide gratings fabrication in silica on silicon technology](#)

J. Vac. Sci. Technol. B **20**, 2085 (2002); 10.1116/1.1510528



physicstoday

Comment on any
Physics Today article.

Physics Today / Volume 63
Previous Article | Next Article
Measured energy in Japan
David von Seggern
(vonneg@seismo.unr.edu) University of Nevada
July 2012, page 10
DIGITAL OBJECT IDENTIFIER
<http://dx.doi.org/10.1063/PT.3.1619>
The article by Thome Lay and Hiroo Kanamori is an estimate of the energy released by the 1994 Chilean earthquake. While that of a 100-megaton nuclear device is approximately five times as much energy as that of a 20-megaton atmospheric explosion, the 1994 Chilean earthquake had still more energy by a factor of about 3, or 15 times as much energy as that of a 100-megaton nuclear device. I believe the authors used the relation for seismic energy release rather than total strain energy release. The seismic energy underestimates the total strain energy release by a variable that depends on friction on the fault plane. Accounting for total strain energy release would increase the earthquake energy number by orders of magnitude.
Despite the catastrophic damage potential of nuclear bombs, the forces of nature occasionally unleash much larger energy releases. Although the nuclear bombs are under our control, earthquakes, volcanic eruptions, and extreme weather events are not. However, by judicious preparation and avoidance measures, humans can significantly diminish the damage of natural events.
This article does not have any references.

Comment on this article
By the act of hitting a ball with a bat, one calculates the force energy to deliver the ball to its new location, but one must also take into account that the bat extended its energy to the struck item, which became struck by the ball as its momentum ceased and passed energy to the struck item. Therefore the parameters of the damage extend into the future when the received energy to that pushed upon, later becomes released in a new event. Perhaps calculations of one added that in while another's calculations did not. E.M.C.
Written by Edgar McCarville, 14 July 2012 19:59

Vertically integrated metal-clad/silicon dioxide-shell microtube arrays for high-spatial-resolution light stimuli in saline

M. Sakata,¹ T. Nakamura,¹ T. Matsuo,¹ A. Goryu,^{1,2} M. Ishida,^{1,3} and T. Kawano^{1,a)}

¹Department of Electrical and Electronic Information Engineering, Toyohashi University of Technology, Toyohashi, Aichi 441-8580, Japan

²Japan Society for the Promotion of Science (JSPS), Chiyoda, Tokyo 102-0083, Japan

³Electronics-Interdisciplinary Research Institute (EIIRIS), Toyohashi University of Technology, Toyohashi, Aichi 441-8580, Japan

(Received 14 January 2014; accepted 6 April 2014; published online 21 April 2014)

Microdevices composed of integrated microscale light source arrays are powerful tools in optogenetic applications. Herein, we prepared vertically aligned 3- μm inner diameter silicon dioxide (SiO_2) tube-based optical light waveguide arrays. To increase the locality of the light stimuli through the tube, we also fabricated metal-cladded SiO_2 tubes using iridium (Ir). After filling the tube with a saline solution, the saline-core/Ir-clad/ SiO_2 -shell waveguide exhibited light stimuli without spreading. With a 532-nm wavelength, the half-power width of the light intensity measured 10 μm above the tube tip was 3 μm , while that of the saline/ SiO_2 -shell waveguide was 9.6 μm , which was more than three times wider. Such high-spatial-resolution optical light stimuli will offer a new class of optogenetic applications, including light stimuli for specific regions of a neuron (e.g., axons or dendrites).

© 2014 AIP Publishing LLC. [<http://dx.doi.org/10.1063/1.4871710>]

Compared to conventional electrophysiological methods, optogenetics,¹ which combines optical and genetics methods (e.g., neuronal activations with channelrhodopsin-2² or inhibition with halorhodopsin), offers a higher spatiotemporal resolution for *in vivo/in vitro* measurements of neurons/cells. Microdevices that consist of both microscale light sources and microelectrode arrays have been fabricated; these devices exhibit simultaneous optical stimulation and electrical recording of neurons/cells.^{3,4} To date, none have demonstrated optical and electrical measurements of neurons/cells using the same alignment within a tissue, although these types of high-spatial-resolution measurements will offer a new class of optogenetics, such as light stimuli and electrical recordings for specific regions of a neuron (e.g., axons or dendrites).⁵ Additionally, it is currently infeasible to fabricate an array of vertical microscale-diameter needle-like waveguides via a standard microfabrication process.

The limitations of conventional microdevices in optogenetics can be overcome by fabricating a vertical tube-like waveguide array. We have fabricated vertically aligned high-aspect-ratio tube arrays of silicon dioxide (SiO_2),^{6,7} and have demonstrated drug delivery⁶ and electrical recording⁷ capabilities using sub-5- μm diameter SiO_2 tube arrays. These microtubes may realize “multifunctional” measurements of neurons/cells in the same alignment.

Here, we show the light stimulating capabilities of a SiO_2 microtube for optogenetic applications with a high spatial resolution. With a light source, including fibers and microscale light emitting diodes (LEDs), placed at the base of the tube, optical signals through the SiO_2 tube can be used for light stimuli (Fig. 1(a)). However, passing through a SiO_2 tube may decrease the locality of the light stimuli and increase the optical crosstalk between the tubes. These performance issues can be addressed by considering the

material of the tube waveguide, such as a high index material like the core or a metal as the clad.^{8,9} To realize a high spatial resolution of optical light stimuli through a SiO_2 tube, herein we fabricate metal-clad/ SiO_2 -shell microtube arrays (Fig. 1(c)). Such high-spatial-resolution optical stimuli can be used for specific regions of a neuron (e.g., axons or dendrites). Although the metal-clad causes optical transmission loss, increasing the input power of the light source (fibers or LEDs) can realize light stimuli with sufficient intensity for optogenetic applications. In the device design, the optical propagation in a saline-filled metal/ SiO_2 microtube is calculated using the finite-difference time-domain (FDTD) method. The effects of the metal clad on the performance of the light stimuli are discussed by comparing to a SiO_2 tube with a same geometry.

The metal layer formed inside a SiO_2 tube acts as the clad for the SiO_2 tube-based waveguide, and using a metal with a smaller resistivity as the clad material increases the optical efficiency.^{8,9} Here, we used Ir (electrical resistivity = 4.71×10^{-9} $\Omega\cdot\text{m}$ at 20 °C) as the clad material because the Ir inside the SiO_2 tube increases the stiffness of the tube (Young’s moduli of SiO_2 and Ir are 75 GPa and 528 GPa, respectively), improving the penetration capability of the tube into a tissue. The other advantage is that Ir has low electrolyte/metal interfacial electrical impedance characteristics. Such a low impedance material formed inside the tube decreases the impedance of a saline-filled tube with a high output/input signal amplitude ratio in electrical recordings of neurons/cells.^{7,10} The penetration and neural recording capabilities of the Ir-clad/ SiO_2 -shell microtube will be discussed in the future.

Optical propagation in a saline/ SiO_2 or saline/Ir/ SiO_2 tube can be analyzed by the FDTD method (Figs. 1(b) and 1(d)). To compare the optical properties between two tubes with the same geometry, the thicknesses of the SiO_2 shell and inside Ir-clad layer of the Ir/ SiO_2 tube were set to 800 nm and 200 nm, respectively (total thickness = 1 μm)

^{a)}Email: kawano@ee.tut.ac.jp. Tel.: +81(532)-44-6738

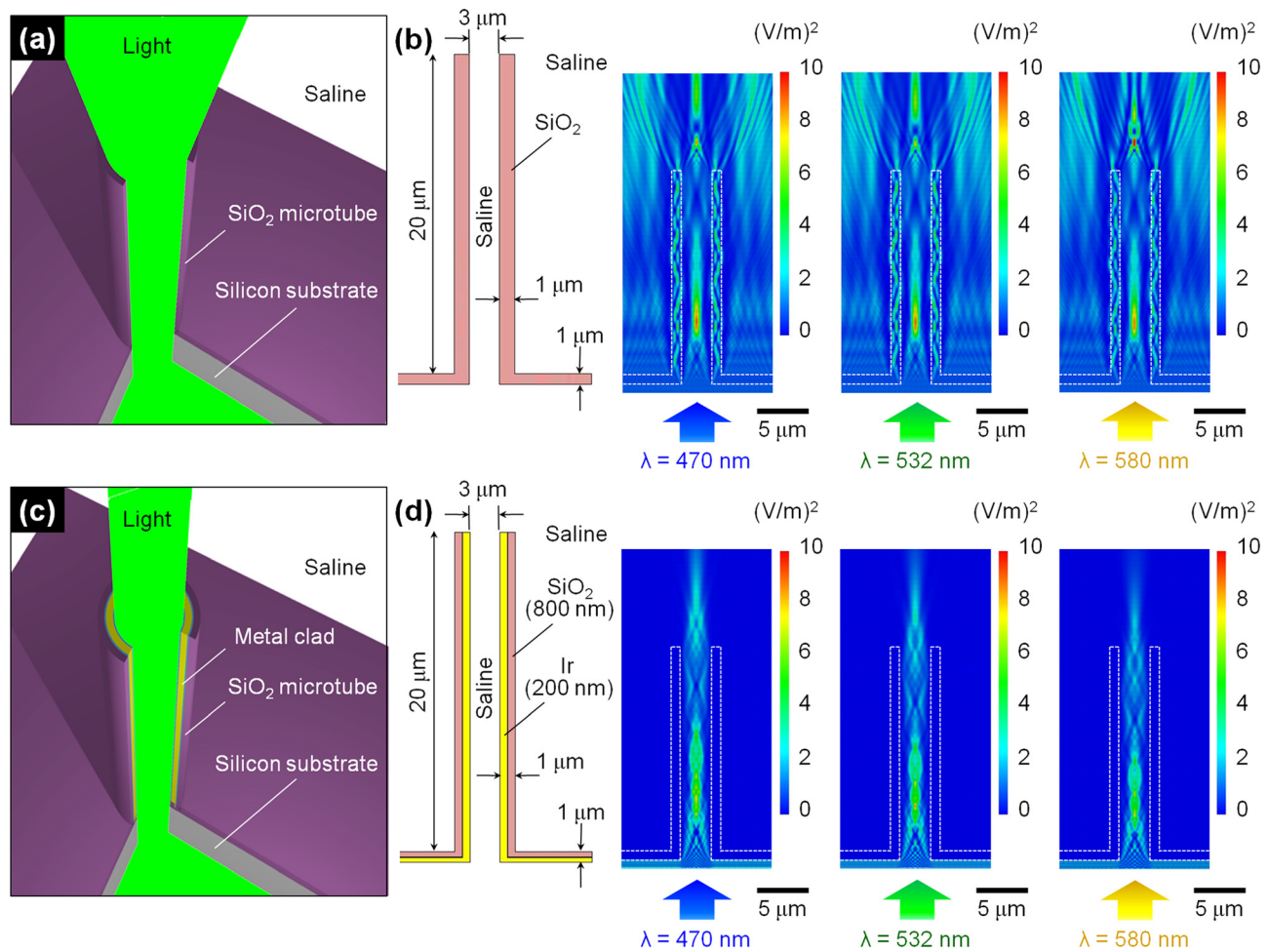


FIG. 1. Light stimulations through SiO₂ and metal-clad/SiO₂-shell tubes in saline for optogenetic applications. (a) Three-dimensional illustration of illumination through a SiO₂ tube with a light source at the tube base. (b) Optical propagations of a saline-filled SiO₂ tube analyzed by the FDTD method. Three FDTD simulations show the optical propagations at wavelengths of 470 nm, 532 nm, and 580 nm. Similar to the actual conditions of a biological tissue, the outer medium is also saline. (c) Illustration for a metal-clad/SiO₂-shell tube. (d) FDTD simulated optical propagations of an Ir-clad/SiO₂-shell tube using the same wavelengths.

(Fig. 1(d)), while the wall thickness of the SiO₂ tube was 1 μm (Fig. 1(b)). To realize a tube with a low invasiveness during tissue penetration,^{11,12} herein the common tube inner diameter was set at 3 μm. The tube length was set at 20 μm, which is sufficient to penetrate numerous thin biological samples, including brain slices (tens to hundreds of microns) and retinae (~200 μm).^{3,13}

For optogenetic applications, we analyzed the optical propagations of each tube using wavelengths of 470 nm for channelrhodopsin-2 and 580 nm for halorhodopsin. Optical propagation using 532-nm wavelength has been used for applications of light stimuli to retinae (e.g., mouse retina³ and gold fish retina¹³). Figures 1(b) and 1(d) show the transverse electric (TE) simulations performed for saline/SiO₂ and saline/Ir/SiO₂ tubes, respectively. The Ir-clad layer improves the locality of light stimuli compared to that of a SiO₂ tube. Note that the refractive indices of SiO₂ (n_{SiO_2}), Ir (n_{Ir}), and saline solution (n_{saline}) varied with wavelength [470 nm ($n_{\text{SiO}_2} = 1.551$, $n_{\text{Ir}} = 1.887 + 3.809i$, and $n_{\text{saline}} = 1.336$), 532 nm ($n_{\text{SiO}_2} = 1.547$, $n_{\text{Ir}} = 2.145 + 4.222i$, and $n_{\text{saline}} = 1.334$), and 580 nm ($n_{\text{SiO}_2} = 1.545$, $n_{\text{Ir}} = 2.357 + 4.441i$, and $n_{\text{saline}} = 1.333$)]. All the light sources modeled in the calculation were plane waves, which represent a laser through an optical fiber placed at the bottom of each tube.

Based on the simulations of optical propagations in the tubes, we fabricated vertically aligned SiO₂- and Ir/SiO₂-microtube arrays (Fig. 2). Fabrication was based on vapor-liquid-solid (VLS) growth of the vertical silicon microwires, subsequent depositions of the Ir and SiO₂ layers, and removal of the core silicon. Initially, a (111) silicon substrate was oxidized to form ~1-μm-thick SiO₂ layer. The substrate was etched by deep reactive ion etching (RIE) from the reverse side in order to form a 150-μm-diameter hole where an optical fiber (125-μm-diameter light source) could be mounted. On the top surface of the silicon substrate, a silicon microwire (3-μm diameter and 30-μm length) was fabricated by Au-catalyzed VLS growth using Si₂H₆-based gas source molecular beam epitaxy (GS-MBE) at a 0.5-Pa gas pressure and a 690 °C growth temperature (Fig. 2(a)).¹⁴ A 200-nm-thick Ir layer with an adhesion titanium (Ti)-layer, which served as the inside metal and device interconnection, was deposited by sputtering and lift-off. The outer shell of 800-nm-thick SiO₂ was deposited over the substrate by plasma-enhanced chemical vapor deposition (PECVD). The wire was then spray-coated with a photoresist, and subsequent plasma etching with O₂ + CF₄ exposed the tip. The SiO₂ and Ir/Ti at the wire tip were etched by a buffered hydrogen fluoride (BHF) solution and RIE. Finally, the core

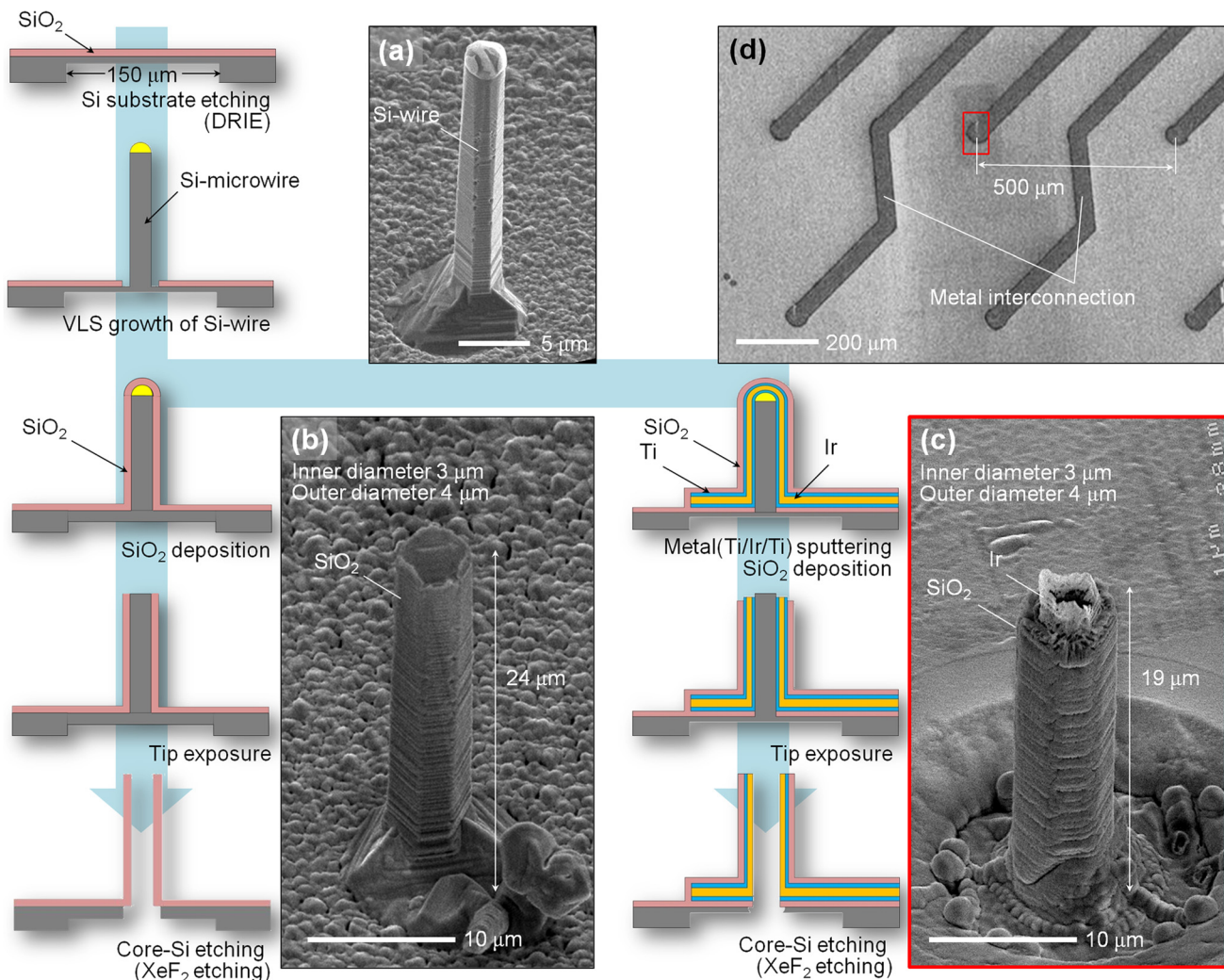


FIG. 2. Fabrication process for both vertical SiO_2 - and Ir-clad/ SiO_2 -shell microtubes. (a) SEM image of a VLS grown silicon microwire. (b) SEM image of a SiO_2 microtube fabricated by deposition of SiO_2 over a silicon wire, exposing the tip section, and etching the core silicon. Inner and outer diameters of a fabricated SiO_2 tube are $3\ \mu\text{m}$ and $4\ \mu\text{m}$, respectively. Tube length is $24\ \mu\text{m}$. (c) SEM image of an Ir-clad/ SiO_2 -shell microtube, which is fabricated by adding Ir/Ti depositions to the fabrication process of SiO_2 tube (b). The fabricated Ir/ SiO_2 tube exhibits the same inner and outer diameters ($3\ \mu\text{m}$ and $4\ \mu\text{m}$). Tube length is $19\ \mu\text{m}$. (d) SEM image of an array of Ir/ SiO_2 tubes integrated with interconnections of Ir/Ti. Red square in the SEM is consistent with the tube shown in (c). Each tube is spaced $500\text{-}\mu\text{m}$ apart.

silicon wire was etched by XeF_2 gas until the tube was connected with the hole on the reverse side. Figure 2(c) shows a SEM image of a fabricated Ir/ SiO_2 microtube with inner and outer diameters of $3\ \mu\text{m}$ and $4\ \mu\text{m}$, respectively. By simply patterning the Ir/Ti layers as an interconnection, each Ir/ SiO_2 microtube could be connected with the device-bonding pad for future applications of multisite electrical recordings of neurons/cells (Fig. 2(d)).⁷ To compare the optical properties, SiO_2 tubes with the same inner and outer diameters were also fabricated by eliminating metal depositions (Fig. 2(b)).^{6,7}

Optical transmissions through the fabricated SiO_2 and Ir/ SiO_2 microtubes were characterized in saline solutions. Herein, the laser light source of an individual tube was an optical fiber ($125\text{-}\mu\text{m}$ diameter) mounted on the reverse side of the substrate through a guide, and the optical signal through the tube was detected using a CCD camera mounted over the tube (Figs. 3(a), 3(b), 3(d), and 3(e)). The wavelength of the laser for the optical transmission tests was $532\ \text{nm}$ because this wavelength is suitable for future applications of optical stimuli to retinae.^{3,13} The transmission rate

of each tube was obtained by measuring the output/input powers with and without placing the tube device between the detector and the fiber, while the common focal point of the detector was set $10\ \mu\text{m}$ above the tube tip. The power of the laser without the microtube device was $2.0\ \text{mW}$. The saline/Ir/ SiO_2 tube exhibited a transmission rate of 0.097% (Figs. 3(d) and 3(e)), while the saline/ SiO_2 tube with the same geometry exhibited a transmission rate of 0.11% (Figs. 3(a) and 3(b)). Although the transmission rate of the saline/Ir/ SiO_2 tube was less than that of the saline/ SiO_2 tube due to absorption in the Ir metal clad,^{8,9} the intensity of the light stimuli increased as the input power of the light source increased. The optical transmission tests also indicated that the area of light stimulation through the saline/Ir/ SiO_2 tube was smaller than that of the SiO_2 tube; these stimulation areas were further examined.

The effect of the Ir clad on the locality of the light stimuli was characterized using the half-power width, which represents the spatial distribution of light at a 50% intensity. Figs. 3(c) and 3(f) show the distributions of the light intensities through saline/ SiO_2 and saline/Ir/ SiO_2 tubes,

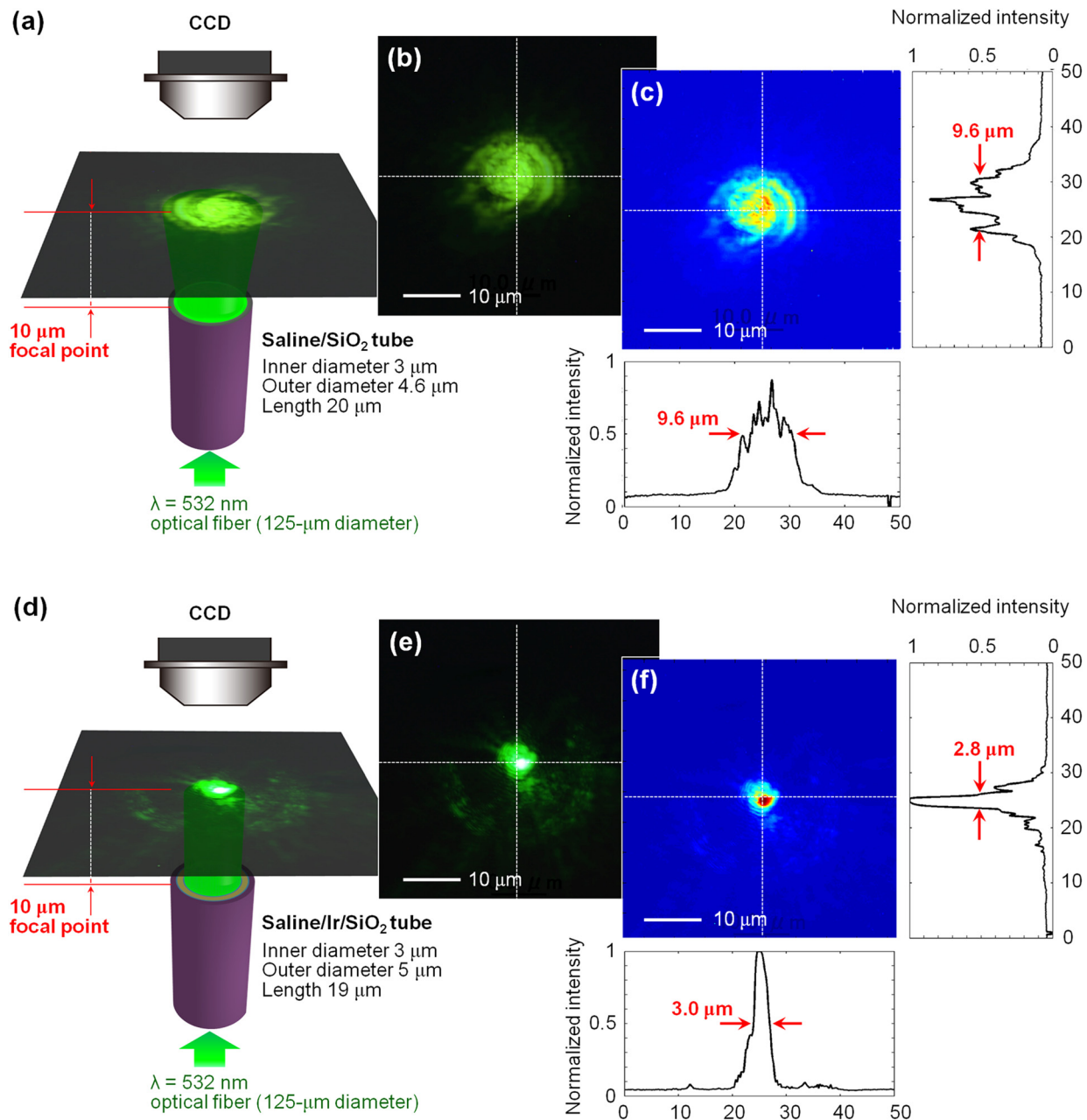


FIG. 3. Optical transmissions through fabricated SiO₂- and Ir-clad/SiO₂-shell microtubes in saline using a laser light source with a wavelength of 532 nm. (a) Schematic of the measurement system for a SiO₂ tube. CCD camera is mounted over the tube. (b) CCD image showing the illumination from the SiO₂ tube. Common focal point of the CCD camera is set 10 μm above the tube tip. (c) Intensity distribution taken from the CCD image (b). Image also includes the normalized intensity—distance curves. (d) Schematic of the measurement system for an Ir clad/SiO₂ tube. (e) CCD image taken at the same focal point (10 μm above the tube tip). (f) Intensity distribution taken from the CCD image (e) including the normalized intensity—distance curves.

respectively, using the CCD camera images shown in Figs. 3(b) and 3(e). The Ir/SiO₂ tube exhibited an improved locality of light stimulation with a half-power-width diameter of 3 μm (Fig. 3(f)), while the SiO₂ tube had a more than three times wider half-power width of 9.6 μm (Fig. 3(c)). The spread of the light through the SiO₂ tube was due to the light through the SiO₂ shell as well as the SiO₂ substrate at the tube bottom (SiO₂ thickness = 1 μm , see Fig. 1(b)). The Ir layer prevented light transmission through the SiO₂ layers (SiO₂ shell and SiO₂ substrate), resulting in light transmission through only the saline-core inside the Ir-clad with an improved half-power-width (3 μm). As confirmed in both the propagation analysis (Figs. 1(b) and 1(d)) and the

transmission tests (Figs. 3(c) and 3(f)), the Ir clad improved the locality of light stimuli.

The intensity of the light stimulation through each tube depended on the input power of the optical fiber. Experiments involving retinae require a sufficient intensity/power of the light to stimulate the retinal photoreceptors.^{3,13} From the transmission tests using an input laser power of 2.0 mW (Fig. 3), the calculated intensity per area through the saline/Ir/SiO₂ tube was 69 mW/mm² within the half-power width (diameter = 3 μm , Fig. 3(f)). This intensity value is sufficient for light stimuli to a retina.¹³ The SiO₂ tube also exhibited a sufficiently high intensity of 8 mW/mm² within the half-power width (diameter = 9.6 μm , Fig. 3(c)).

Although the 532-nm wavelength is suitable for transmission tests in future retinal experiments, the wavelength of the light source (e.g., 470 nm and 580 nm) can be varied for optogenetic applications. Because light sources, including fibers and microscale LEDs, can be set at the base of each tube, numerous wavelengths and input powers can be realized for optogenetic applications.

The fabricated tubes exhibited surface roughness because the films were deposited over the VLS grown silicon-wires with facets (~ 100 nm in roughness). The aforementioned propagation analyses (Figs. 1(b) and 1(d)) employed smooth surface models of SiO₂- and Ir/SiO₂-tubes. The rough surface of the each tube may reduce the intensity of the light stimuli compared to that of the analysis due to the additional transmission loss associated with the scattering at a rough surface (Fig. 3). One way to reduce the surface roughness of the tubes is to use a VLS silicon-wire with a smooth surface, which can be obtained by thermal annealing in hydrogen for an as-VLS grown silicon-wire.¹⁵

In summary, we designed and fabricated vertically aligned microscale-diameter SiO₂- and Ir/SiO₂-tube arrays, and discussed their light stimulation capabilities for optogenetic applications. A comparison between the two types of tubes using FDTD simulations and transmission tests confirmed that the locality of light stimuli is improved through a saline/Ir/SiO₂ tube. Such high-spatial-resolution optical light stimuli to neurons/cells should realize a new class of optogenetic applications (e.g., light stimuli with a microscale spot area in specific regions of a neuron, such as dendrites and axons). In addition, the Ir clad can reduce the electrode impedance inside the SiO₂ tube during electrophysiological recordings,⁷ providing optical and electrical measurements of neurons/cells in the same alignment.

The authors would like to thank Professor Tetsuhiko Harimoto, Professor Hirohito Sawahata, and Professor Rika Numano for their fruitful discussions, Mitsuaki Ashiki and Hiroyuki Takase for their assistance with the fabrication processes, and members at Wakahara Laboratory at Toyohashi Tech for their help with the optical measurements. This work was supported by Grants-in-Aid for Scientific Research (S), Young Scientists (B), and the PRESTO Program from JST. A. Goryu is a recipient of a JSPS fellowship.

¹F. Zhang, A. M. Aravanis, A. Adamantidis, L. Lecea, and K. Deisseroth, *Nat. Rev. Neurosci.* **8**, 577 (2007).

²G. Nage, T. Szellas, W. Huhn, S. Kateriya, N. Adeishvili, P. Berthold, D. Ollig, P. Hegemann, and E. Bamberg, *PNAS* **100**, 13940 (2003).

³J. Zhang, F. Laiwalla, J. A. Kim, H. Urabe, R. V. Wagenen, Y. K. Song, B. W. Connors, F. Zhang, K. Deisseroth, and A. V. Nurmikko, *J. Neural Eng.* **6**, 055007 (2009).

⁴N. Grossman, V. Poher, M. S. Grubb, G. T. Kennedy, K. Nikolic, B. McGovern, R. B. Palmini, Z. Gong, E. M. Drakakis, M. A. A. Neil, M. D. Dawson, J. Burrone, and P. Degenaar, *J. Neural Eng.* **7**, 016004 (2010).

⁵A. M. Packer, D. S. Peterka, J. J. Hirtz, R. Prakash, K. Deisseroth, and R. Yuste, *Nat. Methods* **9**, 1202 (2012).

⁶K. Takei, T. Kawashima, T. Kawano, H. Kaneko, K. Sawada, and M. Ishida, *Biomed. Microdevices* **11**, 539 (2009).

⁷K. Takei, T. Kawano, T. Kawashima, K. Sawada, H. Kaneko, and M. Ishida, *Biomed. Microdevices* **12**, 41 (2010).

⁸C. C. Fesenmaier, Y. Huo, and P. B. Catr, *Opt. Express* **16**, 20457 (2008).

⁹M. K. Kim, A. M. Lakhani, and M. C. Wu, *Opt. Express* **19**, 23504 (2011).

¹⁰S. F. Cogan, *Annu. Rev. Biomed. Eng.* **10**, 275 (2008).

¹¹D. J. Edell, V. V. Toi, V. M. McNeil, and L. D. Clark, *IEEE Trans. Biomed. Eng.* **39**, 635 (1992).

¹²D. H. Szarowski, M. D. Andersen, S. Retterer, A. J. Spence, M. Isaacson, H. G. Craighead, J. N. Turner, and W. Shain, *Brain Res.* **983**, 23 (2003).

¹³M. K. Powers, C. J. Bassi, and P. A. Raymond, *Invest. Ophthalmol. Visual Sci.* **29**, 37 (1988).

¹⁴A. Ikeda, T. Kawashima, T. Kawano, and M. Ishida, *Appl. Phys. Lett.* **95**, 033502 (2009).

¹⁵M. C. M. Lee and M. C. Wu, *J. Microelectromech. Syst.* **15**, 338 (2006).